

The Morphology, Crystallography, and Chemistry of Phases in As-Cast Nickel-Aluminum Bronze

F. HASAN, A. JAHANAFROOZ, G. W. LORIMER, and N. RIDLEY

The morphology, crystallography, and composition of the phases present in as-cast nickel-aluminum bronze of nominal composition copper-10 wt pct aluminum-5 wt pct nickel-5 wt pct iron have been investigated using optical, electron optical, and microprobe analysis techniques. The as-cast microstructure consists of copper-rich α , martensitic β , and κ -phases based on Fe_3Al and NiAl . The κ_I precipitates have a dendritic morphology and are cored; the composition ranges from iron-rich solid solution to Fe_3Al . The κ_{II} and κ_{IV} precipitates have, respectively, a dendritic and an equiaxed/dendritic morphology, and are based on Fe_3Al , while κ_{III} is a eutectoidal decomposition product of lamellar or globular morphology based on NiAl . The κ_I , κ_{II} , and κ_{III} precipitates have the Kurdjumov-Sachs orientation relationship with α matrix. Small κ_{IV} precipitates exhibit the Nishiyama-Wasserman orientation relationship with the α matrix, while large κ_{IV} precipitates have an orientation relationship which lies between Kurdjumov-Sachs and Nishiyama-Wasserman.

I. INTRODUCTION

NICKEL-aluminum bronze (NAB) with a nominal composition Cu-10 wt pct Al-5 wt pct Ni-5 wt pct Fe is widely used to produce cast components for marine applications. However, the alloy shows a variable resistance to corrosion in sea water, and this has been attributed to the complex microstructure which is affected by the thermal history of the casting and by its chemical composition.

Under normal casting conditions, the alloy has a microstructure consisting of an fcc Cu-rich solid solution or α -phase, several intermetallic phases collectively referred to as κ -phase, and some "retained β -phase". Figure 1 shows the phase-relationships in the Cu-Al-Ni-Fe quaternary system at 5 wt pct Ni and 5 wt pct Fe, as determined by Cook *et al.*¹ The work of Cook *et al.*¹ suggested that the κ -phase was an Ni-Fe-Al complex with an ordered bcc (B2) structure. Weill-Couly and Arnaud² classified the κ -phases into four types on the basis of the various morphologies observed in the optical microscope. Recently, microstructural studies have been made using electron beam instruments, and some information about the chemistry of the κ -phases has been obtained by the microanalysis of both bulk and thin specimens.^{3,4}

The object of the present work was to investigate the crystal structures of the various κ -phases (precipitates), to determine their orientation relationships with the α -matrix, and to examine their chemical compositions. The microanalysis and diffraction data have been combined to produce a classification of the κ -phases based on their chemistry and crystallography, rather than on morphology alone.

II. EXPERIMENTAL

The compositions of the alloys examined, as determined by wet chemical analysis, are given in Table I. Most of the investigation was concentrated on Alloy I and the results are

F. HASAN and A. JAHANAFROOZ, Graduate Students, and G. W. LORIMER and N. RIDLEY, Senior Lecturers, are all with Joint University of Manchester/UMIST, Department of Metallurgy, Grosvenor Street, Manchester M1 7HS, England.

Manuscript submitted September 23, 1981.

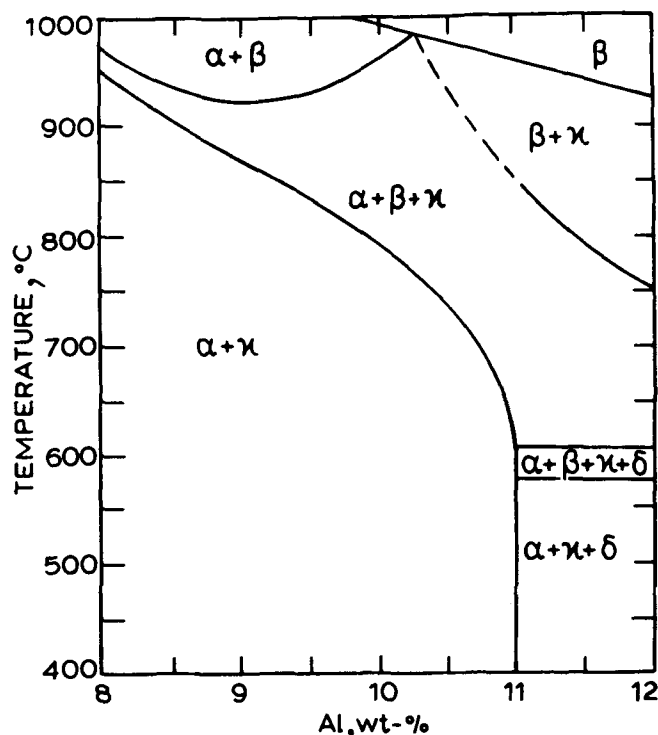


Fig. 1 — Vertical section of the Cu-Al-5Ni-5Fe equilibrium diagram, after Cook *et al.*¹

Table I. Chemical Composition of Alloys, Wt Pct

Elements	Cu	Al	Ni	Fe	Mn	Si
Alloy - I	80.0	9.4	4.9	4.4	1.2	0.07
Alloy - II	80.1	9.0	4.4	5.1	1.4	0.07

from this alloy unless stated otherwise. For optical microscopy the specimens were polished using conventional procedures and etched in a solution of 10 pct ferric nitrate in water. Carbon extraction replicas of polished and etched specimens were prepared using standard techniques. Thin foil specimens were prepared either by electropolishing in 7 pct perchloric acid in acetic acid at room temperature using a potential of 30 volts, or by ion-beam-thinning with

5.5 kV argon ions in an Ion Tech Super Microlap apparatus. Electron microscopy of thin foils and surface replicas was carried out with either Philips EM301 or EM400T transmission electron microscopes.

The microanalyses of various phases/precipitates were carried out with either bulk or thin specimens. The analyses of large precipitates (κ_1) which were carried out in bulk specimens, subsequently referred to as bulk microprobe analyses, were made on a Cambridge S180 scanning electron microscope fitted with an energy dispersive X-ray detector. The microanalyses of thin foils and extracted thin precipitates, subsequently referred to as thin specimen microprobe analyses, were carried out on a Philips EM400T analytical electron microscope fitted with an EDAX energy dispersive X-ray detector and ancillary electronics. These analyses were carried out with the instrument operating in the TEM mode with a probe size of approximately 100Å.

Quantitative chemical analyses were obtained from thin specimens using procedures discussed in detail elsewhere.^{4,5} In brief, this involved converting the observed X-ray intensity ratios I_A/I_B into weight fraction ratios C_A/C_B using the relationship

$$C_A/C_B = k_{AB}I_A/I_B \quad [1]$$

where k_{AB} is a constant at given voltage which can be determined experimentally or calculated.⁵ During the present investigation the k_{AB} values were calculated. These values agreed well with k_{AB} values which had been obtained experimentally in our laboratory over a period of years. We estimate the error in our k_{AB} values to be ± 2 pct. A normalization procedure was used to convert the weight fraction ratio of each element, C_n , into a weight percentage, *i. e.*, $\sum C_n = 1$.

X-ray absorption within the specimen can affect the observed X-ray intensity ratio when the X-rays have different energies, *e. g.*, Al K_α compared to Fe or Ni K_α radiation. Corrections for the effects of absorption within the specimen were made using the expression

$$\frac{I_A}{I_B} = \frac{I_{0A}\mu_B(1 - e^{-\mu_A\rho t \csc\theta})}{I_{0B}\mu_A(1 - e^{-\mu_B\rho t \csc\theta})} \quad [2]$$

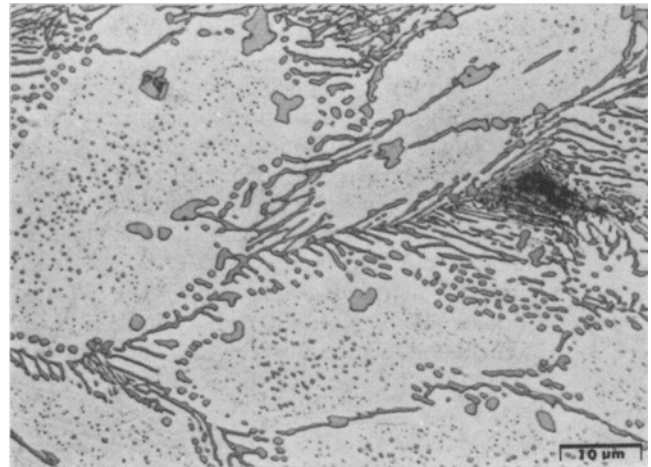
where I_A/I_B is the observed X-ray intensity ratio, I_{0A}/I_{0B} the X-ray intensity ratio that would be observed in the absence of absorption, t the thickness at the point of analysis, μ_A and μ_B the X-ray absorption coefficients in the specimen, θ the angle between the center line of the detector and the sample surface, and ρ the sample density. Since μ_A , μ_B , and ρ are functions of composition it is necessary to use an iterative procedure to calculate the ratio I_{0A}/I_{0B} .

Thickness values were obtained by using a simple parallax technique in which the relative movement, during a tilt of ± 45 deg, of details on the top and bottom of the specimen were measured. In practice, the thickness range, at the point of analysis, varied between 500 to 800Å. It was possible to determine the thickness with sufficient accuracy to limit the total relative error in calculated weight percentages (using Eq. [2]) to typically ± 10 pct.

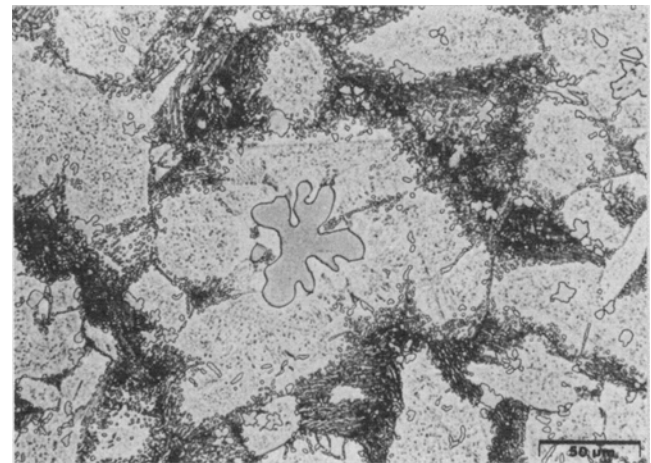
Lattice parameter measurements were obtained from electron diffraction patterns taken from samples which had been sputter-coated with a thin layer of gold. The gold rings provided a standard on each diffraction pattern and enabled lattice parameter data to be obtained which was accurate to ± 1 pct.

III. RESULTS

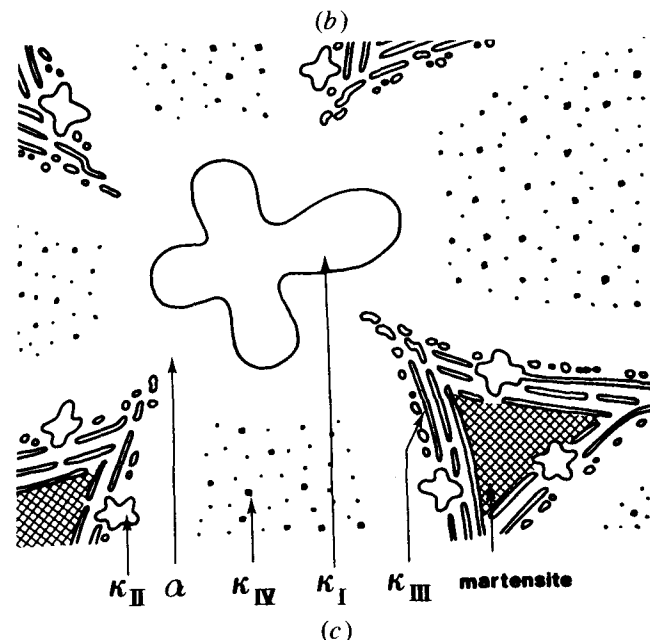
The microstructure of the as-cast NAB is shown in Figure 2 and the various features are identified below.



(a)



(b)



(c)

Fig. 2—Micrographs of cast NAB showing (a) the phase distribution in Alloy I, (b) a large κ_1 particle in Alloy II, and (c) schematic representation of the distribution of phases in cast NAB.

A. α -Phase

The white-etching areas in Figures 2(a) and 2(b) are the Cu-rich fcc α -phase, which has a lattice parameter of $3.64 \pm 0.04\text{\AA}$. The chemical composition of the α -phase, as determined from the matrix in thin foil specimens, is about 85 wt pct Cu-7 wt pct Al-3 wt pct Ni-3 wt pct Fe, and 1 wt pct Mn (Table II).

B. κ -Phases

The large, dendritic-shaped particle shown in Figure 2(b) is a κ_I precipitate. These particles were observed only in Alloy II, which has a higher iron content (Table I). The κ_I particles were always located in the centers of α grains (Figure 2(b)), and were typically 20 to 50 μm in diameter. Bulk microprobe analyses of these precipitates indicate that they are iron-rich with less than 25 wt pct Al (Table II). The central portions of κ_I contain small Cu-rich precipitates (Figure 3). The κ_I particles do not exhibit a single crystal structure; each particle is composed of a number of different structures including disordered iron-rich solid solution (bcc), Fe_3Al (DO_3), and FeAl (B2). Some of the electron diffraction patterns obtained from κ_I particles are shown in Figure 4.

The κ_{II} precipitates are the smaller, 5 to 10 μm diameter, dendritic-shaped particles many of which occur in the regions which contain the lamellar eutectoid decomposition product (Figure 2). Thin specimen microprobe analyses (Table II) of individual κ_{II} precipitates indicate that they are based on Fe_3Al with nickel, copper, and manganese substituting for iron, and silicon for aluminum. Electron diffraction patterns from the κ_{II} precipitates (Figure 5) indicate that they have the DO_3 Schnoeflies (cF4 Pearson) structure and a lattice parameter of $5.71 \pm 0.06\text{\AA}$.

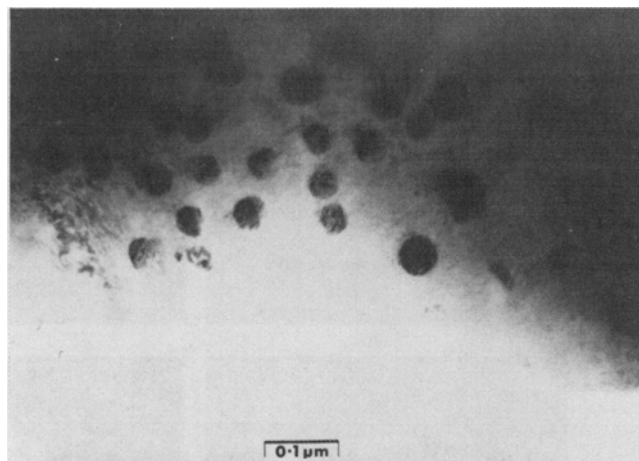


Fig. 3—Cu-rich precipitates in κ_I (transmission electron micrograph).

The κ_{III} precipitates are lamellar or globular (degenerate lamellar) eutectoid decomposition products. Electron diffraction patterns (Figure 5) and thin specimen microprobe analyses (Table II) from individual extracted lamellae show that κ_{III} has the B2 structure based on NiAl , with a lattice parameter of $2.88 \pm 0.03\text{\AA}$, and with iron, copper, and manganese substituting for nickel.

The small precipitates distributed throughout the α -grains (Figure 2) which show a range of sizes (Figure 6(a)) are the κ_{IV} particles. A precipitate free zone (PFZ) exists at the periphery of the α -grains. Some of the κ_{IV} particles are internally twinned (Figure 6(b)). Thin specimen microprobe analyses (Table II) and electron diffraction (Figure 5) of extracted individual κ_{IV} particles indicate that they have a composition and crystal structure similar to κ_{II} ;

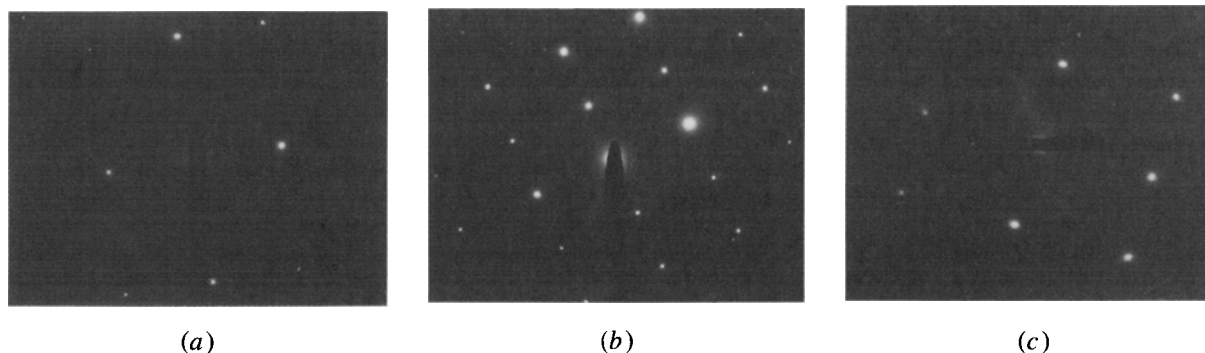


Fig. 4—Electron diffraction patterns along $\langle 110 \rangle$ zone axis from κ_I precipitates: (a) bcc: iron-rich solid solution, (b) DO_3 (Fe_3Al), and (c) B2 (FeAl).

Table II. Chemical Analyses (Wt Pct*) of Phases in Cast NAB. Atomic Percent Composition in Brackets

Phases	Number of Analyses	Technique	Al	Si	Mn	Fe	Ni	Cu
κ_I (Alloy-II)	12	bulk	9.3 ± 0.5 (17.5)	1.6 ± 0.4 (2.9)	2.9 ± 0.5 (2.7)	72.2 ± 1.4 (65.6)	3.5 ± 0.4 (3.0)	10.5 ± 1.0 (8.4)
κ_{II}	10	thin foil	12.3 ± 1.3 (22.2)	4.1 ± 0.8 (7.1)	2.2 ± 0.2 (1.9)	61.3 ± 4.9 (53.0)	8.0 ± 1.8 (6.6)	12.1 ± 3.1 (9.3)
κ_{III}	10	extraction replica	26.7 ± 1.0 (44.3)	<0.1	2.0 ± 0.4 (1.6)	12.8 ± 1.6 (10.2)	41.3 ± 6.0 (31.5)	17.0 ± 4.6 (12.0)
κ_{IV}	12	extraction replica	10.5 ± 1.7 (18.9)	4.0 ± 0.5 (6.9)	2.4 ± 0.2 (2.1)	73.4 ± 2.3 (63.8)	7.3 ± 1.5 (6.1)	2.6 ± 0.7 (2.0)
Particles in β	10	extraction replica	28.1 ± 0.8 (46)	0.4 ± 0.3 (0.6)	2.2 ± 0.3 (1.8)	14.0 ± 6.0 (11.0)	35.1 ± 8.6 (26.4)	20.2 ± 3.7 (14.1)
α	8	thin foil	7.2 ± 0.4	<0.1	1.1 ± 0.1	2.8 ± 0.3	3.0 ± 0.2	85.8 ± 0.4

*Wt pct \pm one standard deviation

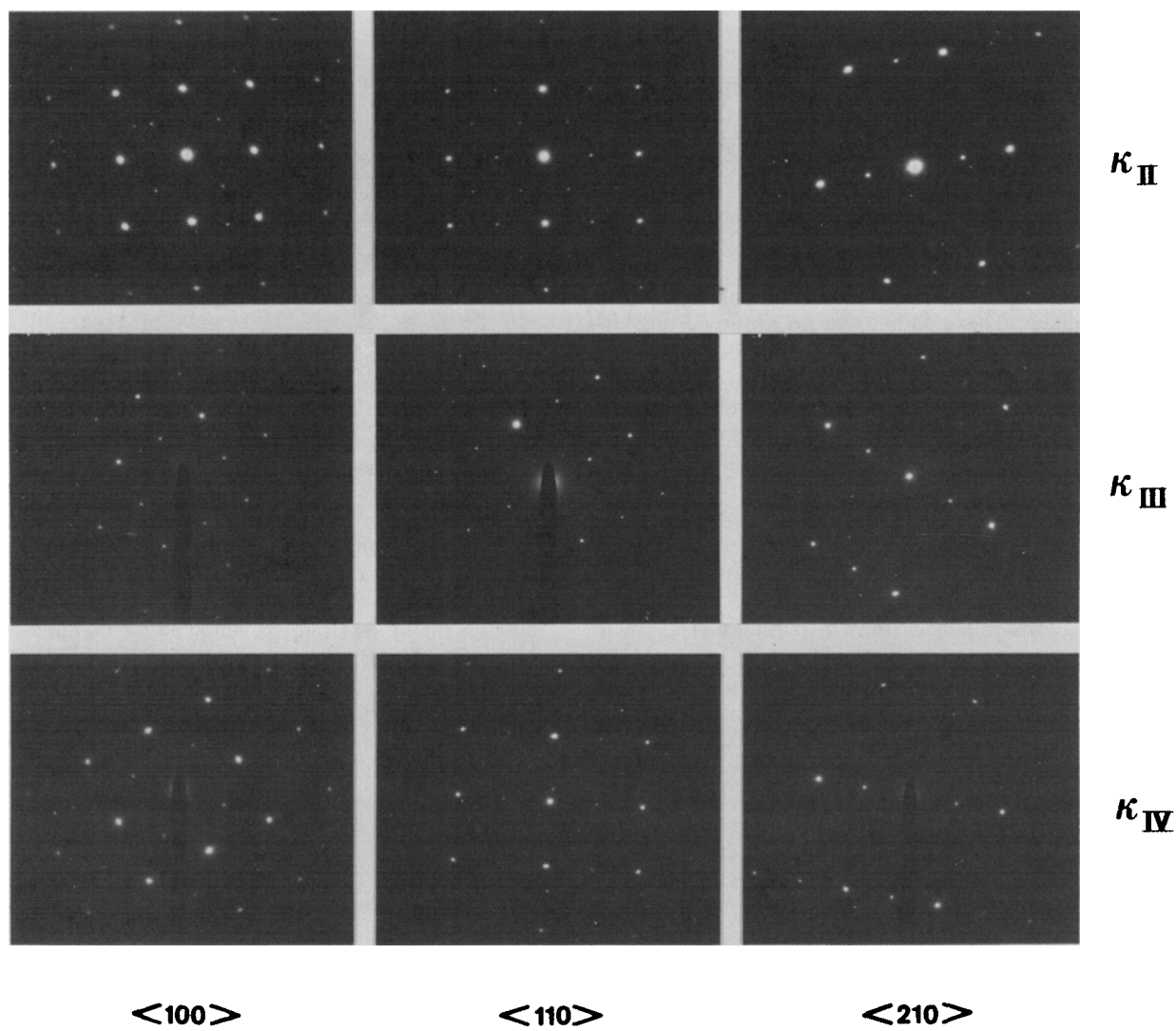
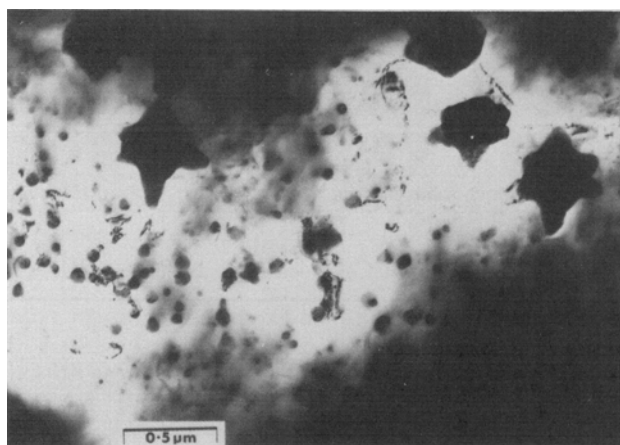


Fig. 5—Electron diffraction patterns from single κ particles obtained along $\langle 100 \rangle$, $\langle 110 \rangle$, and $\langle 210 \rangle$ zone axes.



(a)



(b)

Fig. 6—Transmission electron micrographs of a thin foil specimen showing (a) κ_{IV} particles of various sizes and (b) internally twinned κ_{IV} particles.

they are based on Fe₃Al and have a lattice parameter of $5.77 \pm 0.06 \text{ \AA}$.

C. "Retained- β "

The dark etching intergranular regions in cast Ni-Al bronze (Figure 2) are traditionally referred to as "retained- β ",^{2,6} although it is acknowledged that the high temperature phase will have undergone some change upon cooling to room temperature.² Culpan and Rose³ suggested that "retained- β " had a complex structure and should be described as β' to distinguish it from the high temperature phase.

Transmission electron microscopy (Figure 7(a)) shows that the "retained- β " is martensite. Electron diffraction patterns of the martensite in as-cast specimens can be indexed as either 3R (Figure 7(b)) or 2H martensite.⁷ The 3R martensite contains a high density of precipitates (Figure 7(c)), the size of which depends on the cooling rate. Electron diffraction patterns taken from individual precipitates or large numbers of precipitates which had been extracted on carbon films (Figure 7(d)) can be indexed as the B2 structure (DO₁₉ (Schnoeflies) or cP2 (Pearson)) with a lattice parameter of $2.85 \pm 0.03 \text{ \AA}$. Thin specimen microprobe analyses of these precipitates indicate that they are based on NiAl (Table II).

D. Orientation Relationships between the κ -Precipitates and the α -Matrix

The orientation relationships between the various κ precipitates and the α -matrix were determined from electron diffraction patterns taken from thin foil specimens, and these are shown in Figures 8 and 9. The κ_I , κ_{II} , and κ_{III} precipitates all exhibit the Kurdjumov-Sachs orientation relationship with the α -matrix (Figure 8):

$$\begin{aligned} [011]_{\kappa} &\parallel [111]_{\alpha} \\ [11\bar{1}]_{\kappa} &\parallel [10\bar{1}]_{\alpha} \\ [\bar{2}1\bar{1}]_{\kappa} &\parallel [\bar{1}2\bar{1}]_{\alpha} \end{aligned}$$

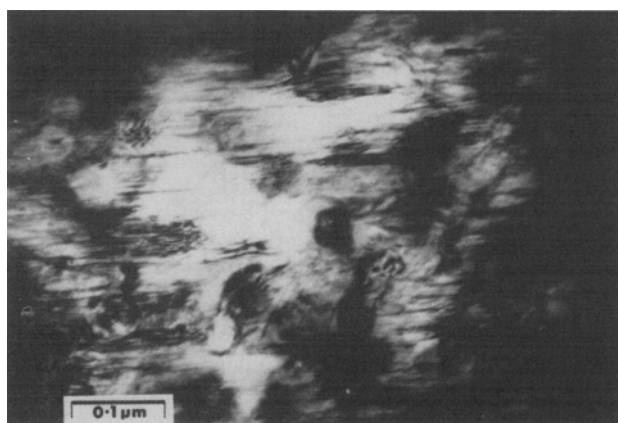
and

The κ_{IV} particles exhibit a more complicated behavior. Smaller particles have the Nishiyama-Wasserman orientation relationship with the α -matrix (Figure 9):

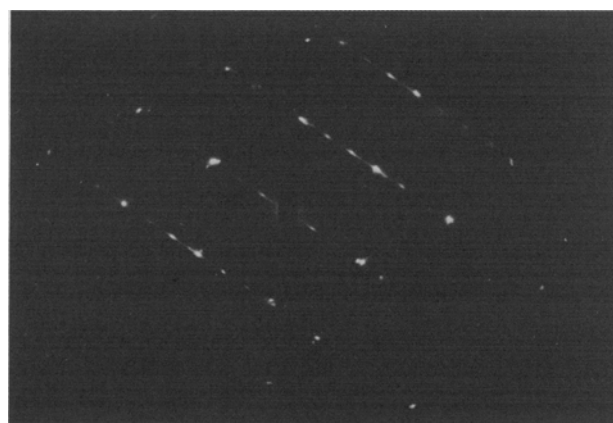
$$\begin{aligned} [001]_{\kappa} &\parallel [001]_{\alpha} \\ [\bar{1}10]_{\kappa} &\parallel [\bar{1}11]_{\alpha} \\ [110]_{\kappa} &\parallel [21\bar{1}]_{\alpha} \end{aligned}$$

and

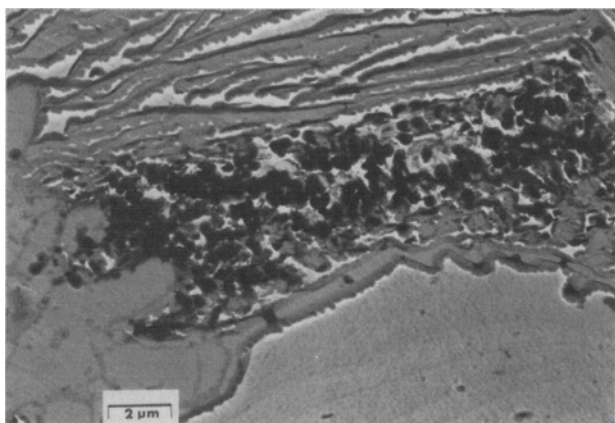
while larger κ_{IV} particles have an orientation relationship which lies between the Nishiyama-Wasserman and Kurdjumov-Sachs orientation relationships.



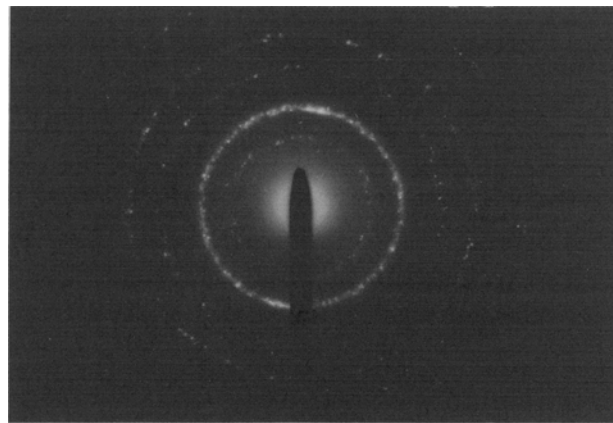
(a)



(b)



(c)



(d)

Fig. 7—(a) Transmission electron micrograph of the "retained β " region showing martensite. The particles are NiAl. (b) Electron diffraction pattern from the martensite matrix which can be indexed as a 3R structure. (c) Fine precipitates extracted from the martensite in (a). (d) Electron diffraction ring pattern from (c), which can be indexed as a B2 (NiAl) structure.

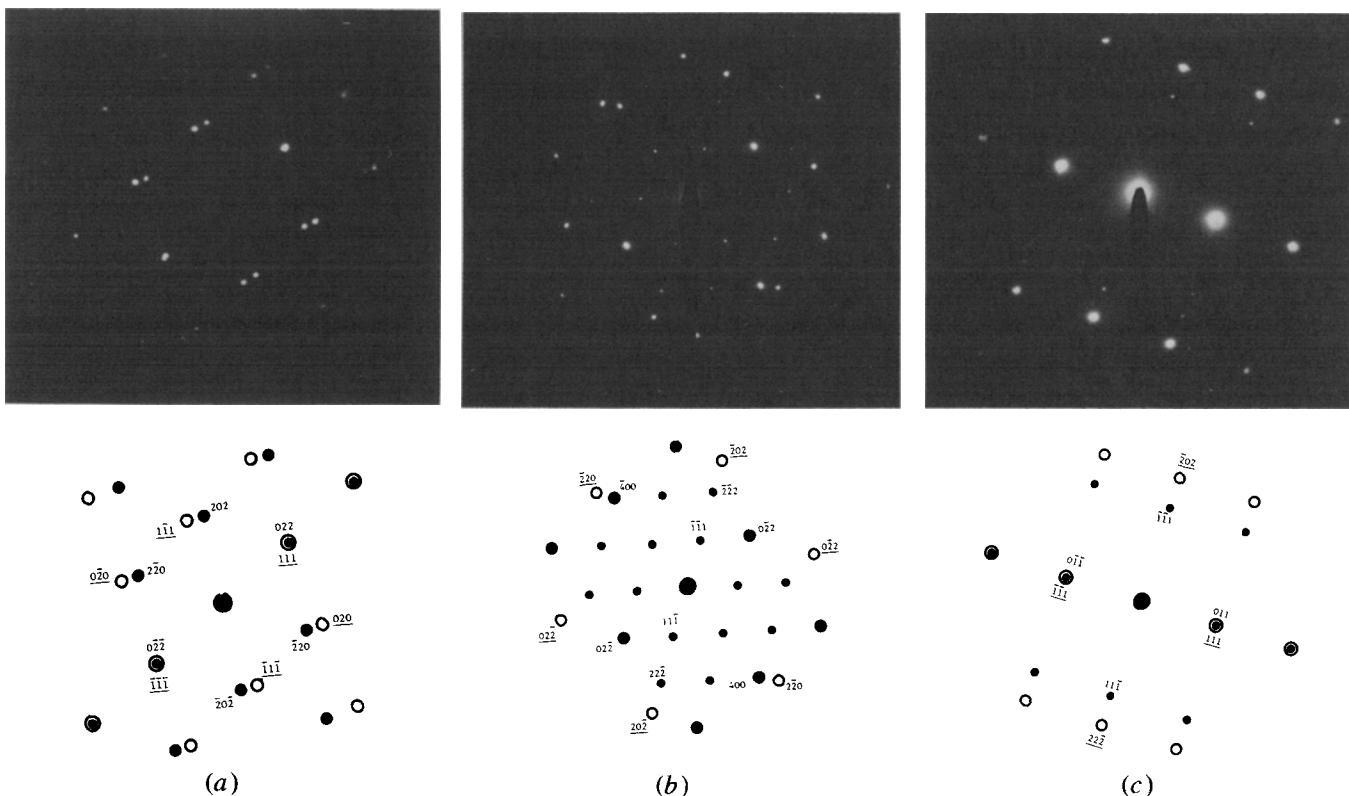


Fig. 8—Electron diffraction patterns showing the Kurdjumov-Sach (K-S) orientation relationship between the matrix and (a) κ_I , (b) κ_{II} , and (c) κ_{III} precipitates. (○ hkl matrix, ● hkl precipitate)

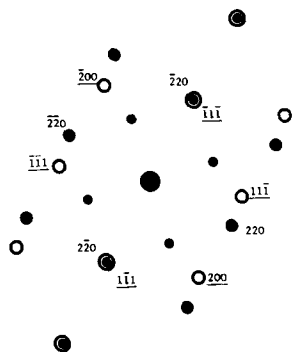


Fig. 9—Electron diffraction pattern illustrating the Nishiyama-Wasserman (N-W) orientation relationship between the matrix and small κ_{IV} precipitates. (○ hkl matrix, ● hkl precipitate)

IV. DISCUSSION

A. The Distribution and Morphology of Phases

Under normal rates of cooling, cast NAB contains an fcc Cu-rich solid solution or α -phase, some “retained β ”, and numerous intermetallic precipitates collectively referred to as κ -phase. The precipitates have a dendritic, spheroidal, or lamellar morphology. These various morphologies have been designated as distinct phases by Weill-Couly and Arnaud,² and their classification has become established in the literature. In the present work the distribution of precipitates (phases), as seen in the optical microscope (Figure 2), differs significantly from the classification of Weill-Couly and Arnaud.² The present observations are shown schematically in Figure 2(c).

The differences between the distribution of κ -precipitates shown in Figure 2(c) and that of Weill-Couly and Arnaud² concern the position of κ_I relative to other phases, and also the morphology of κ_{IV} . Weill-Couly and Arnaud² indicated that κ_I was located in the eutectoid or in retained β regions, whereas in the present work κ_I was always found in the α . The κ_{II} is frequently observed within the eutectoid decomposition product, and large κ_{II} particles may be mistaken for κ_I ^{3,6} if the Weill-Couly and Arnaud² classification is adopted. The κ_{IV} precipitates, when viewed optically, always appear as small $<2 \mu\text{m}$ diameter, equiaxed particles, whereas Weill-Couly and Arnaud² have described κ_{IV} as having either an equiaxed or a rhombohedral morphology.

The present classification agrees, for the most part, with the work of Culpan and Rose³ and Rowlands and Brown,⁶

except where these authors have identified κ_{II} particles as κ_I , on the basis of the Weill-Couly and Arnaud classification as discussed above.

B. The Crystal Structure and Chemistry of the κ Phases

The microprobe analyses (Table II) and electron diffraction data shown in Figure 5 indicate that in Alloy I there are two chemically and structurally distinct κ -phases; one based on Fe_3Al and the other on $NiAl$. The κ_{II} and κ_{IV} precipitates are based on Fe_3Al with $Fe (+Ni+Cu+Mn) = 65$ to 75 at. pct and $Al(+Si) = 25$ to 35 at. pct, while κ_{III} is based on $NiAl$ with iron, copper, and manganese substituting for nickel. This result agrees with the proposal of Weill-Couly and Arnaud² that κ_I , κ_{II} , and κ_{IV} particles are Fe-rich while the lamellar eutectoid decomposition product, κ_{III} , is Ni-rich. The present results show that κ_{II} and κ_{IV} have the same chemistry and structure and should not be designated as separate phases. The earlier proposal of Cook *et al.*¹ that the κ -phases are based on a single Ni-Fe-Al complex with the B2 structure is clearly incorrect. Likewise, the present studies do not support the work of Thomson and Edwards⁸ in which they postulated, on the basis of chemical analysis and of X-ray diffraction studies on chemically extracted residues, that both the Fe-rich (based on Fe_3Al) and Ni-rich (based on $NiAl$) morphologies were two extremes of the same phase and that they were isostructural. The chemical analyses reported by Culpan and Rose³ and Lloyd *et al.*⁴ are similar to those found in the present work.

The crystal structures of $NiAl$ and Fe_3Al are shown schematically in Figure 10. Eight unit cells of the $NiAl$ structure have been drawn to emphasize the similarity of the two structures. In $NiAl$ all of the body-centered positions are occupied by aluminum, while in Fe_3Al half of these positions are occupied by transition elements, in a tetrahedral arrangement, and the other half is filled by aluminum (+ silicon) atoms. The structure and the relationship between them is discussed in detail by Barrett and Massalski.⁹ The similarity of the two structures is reflected in the diffraction patterns shown in Figure 5. When the lattice parameters of the two phases differ by a factor of two, as in

the present situation, it is necessary to compare electron diffraction taken along selected directions, *e. g.*, [110] or [211], to differentiate between the two structures.

Although comprehensive information is not available in the literature concerning the phase relationships in the Cu-Al-Fe-Ni quaternary system, it is possible to comment on the potential composition range of the Fe_3Al and $NiAl$ intermetallic phases by referring to the relevant ternary phase diagrams as determined by Bradley, Bragg, and Sykes.¹⁰ Figure 11 is taken from their work on alloys slow-cooled to room temperature, and the ternary sections have been arranged so as to emphasize the interrelationship between the $NiAl$ and Fe_3Al phase fields.

According to Figure 11, the Fe_3Al phase (labeled as β_1) can contain 25 to 35 at. pct Al, and a limited amount of iron can be substituted by nickel and copper atoms. The $NiAl$ phase (labeled as β_2) exhibits a wide composition range; the nickel content can be substantially replaced by iron or copper and a large variation in the aluminum content is possible. In fact, the β_2 phase field extends across the diagram to include both $NiAl$ and $FeAl$. However, since the composition of κ_{III} is always closer to $NiAl$ it seems reasonable

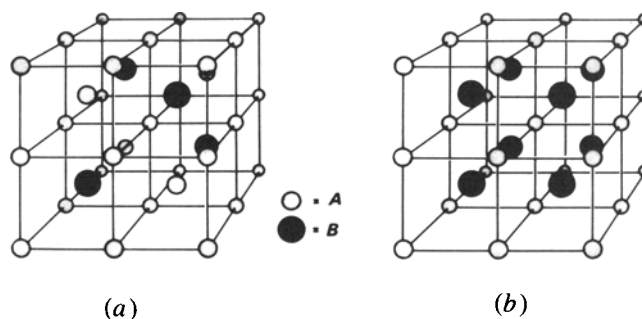


Fig. 10—Schematic representation of the crystal structures of the κ -phases: (a) Fe_3Al structure of κ_{II} and κ_{IV} . The positions A are occupied by $Fe (+Ni+Cu+Mn)$ and positions B by $Al (+Si)$. (b) $NiAl$ structure of κ_{III} phase. The positions A are occupied by $Ni (+Fe+Cu+Mn)$ and positions B by Al . Eight unit cells of $NiAl$ structure are shown to illustrate its similarity with Fe_3Al .

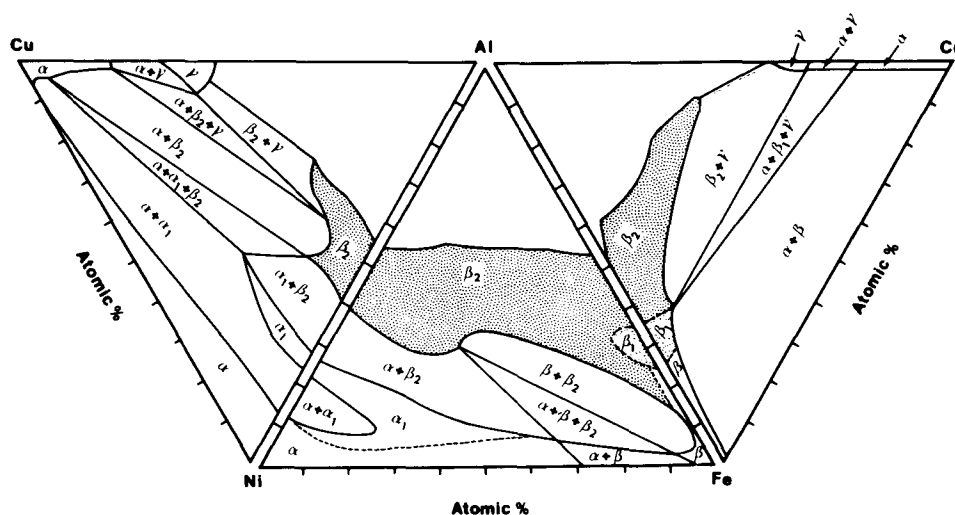


Fig. 11—Sections of Cu-Ni-Al, Ni-Fe-Al, and Fe-Cu-Al ternary equilibrium diagrams, after Bradley, Bragg, and Sykes,¹⁰ arranged so as to illustrate the composition range of intermetallic phases based on $NiAl$ and Fe_3Al in cast NAB. The details in the Al-rich corner have been omitted.

to describe κ_{III} as NiAl rather than NiAl-FeAl as has been previously suggested.^{3,6}

The chemical compositions of κ_{II} , κ_{III} , and κ_{IV} in at. pct (Table II) indicate that the deviations from the exact stoichiometric proportions exhibited by κ -phases are in accordance with the ternary diagrams (Figure 11). The mutual replacement of iron and nickel, and the extent to which both of them can be replaced by copper, is also consistent with the ternary sections.

The relationship between the chemistry and structure of κ_I cannot be fully explained with the help of Figure 11. The major complication is that κ_I is not an equilibrium phase, but is cored. According to Figure 11 κ_I which contains less than 25 at. pct Al should have a bcc structure, or it can have a B2 structure when more than 2.5 at. pct Ni is present. However, recent investigations of binary Fe-Al alloys with compositions in the region of Fe₃Al indicate that the phase relationships are extremely complex.^{11,12,13} The iron-aluminum solid solution forms a series of ordered structures whose existence depends on composition, temperature, and prior thermal history. The formulas Fe, Fe₇Al, Fe₁₃Al₃, Fe₃Al, and FeAl have been used to describe these structures. It has also been suggested that these "formula states" may be regarded as structural transitions of ordering with increasing aluminum contents.¹¹ In the alloys under investigation the presence of nickel and copper and a variable cooling rate increase the complexity even further.

C. The "Retained β " Phase

Examination of the foil specimens (Figure 7) has revealed that the "retained β " regions are composed of martensite containing small particles based on NiAl. The existence of 3R and 2H-type martensite has been confirmed by electron diffraction. The NiAl particles within the martensite generally have a spherical or cubic morphology. The adverse effect that the "retained β " has on the corrosion resistance of the cast alloy has led many workers to propose that there may be some γ_2 phase (or δ) associated with the "retained β " regions.¹⁴ During the present work no γ_2 was observed in the microstructure. However, it is possible that the high chemical reactivity of the metastable martensite phase may be responsible for the accelerated corrosion of these regions.

D. Tempering at 675 °C

To improve the corrosion resistance, the cast alloy may be given a tempering treatment at 675 °C for two to six hours. The treatment results in the formation of fine precipitates inside the α -grains. Culpan and Rose³ have studied these fine precipitates by scanning microscopy. They reported that there were two types of precipitates, one rich in nickel and the other rich in iron. During the present investigation, transmission and analytical electron microscopy of surface replicas and thin foils has revealed that the fine precipitates which form during tempering have the B2 structure and are based on NiAl. Details of this investigation will be presented elsewhere.¹⁵

E. Orientation-Relationships

The orientation relationships of the various κ morphologies with the fcc matrix have been studied in the present work. It has been observed that κ_I , κ_{II} , and κ_{III} have

the Kurdjumov-Sachs (K-S) orientation relationships with the matrix, shown in Figure 8. The κ_{IV} particles, however, show a complicated behavior. The very small κ_{IV} particles have a Nishiyama-Wasserman (N-W) type relationship with the matrix (Figure 9), while the larger particles exhibit an orientation relationship with the matrix which is somewhere between Nishiyama-Wasserman and Kurdjumov-Sachs. This variation in orientation relationship with particle size is thought to be associated with the internal twinning of the larger κ_{IV} particles.

It might be expected that κ_{II} and κ_{IV} , which are both based on Fe₃Al, would have the same orientation relationship with the α matrix. However, κ_{IV} nucleates directly in the α phase, whereas κ_{II} nucleates at relatively high temperatures in the pre-existing β -phase and is enveloped by the precipitating α -phase during cooling. The orientation of κ_{II} relative to the α phase is therefore dependent on its original orientation relationships with the β phase.

V. SUMMARY

The morphology, crystallography, and composition of the phases present in as-cast nickel-aluminum bronze have been determined.

The as-cast microstructure consists of copper-rich α phase, "retained β ", and various precipitates, collectively referred to as κ -phase, based on Fe₃Al or NiAl. The fcc α -matrix has an approximate composition of copper-7 wt pct aluminum-3 wt pct nickel-3 wt pct iron. Regions of the high temperature bcc β phase which do not undergo diffusional decomposition on cooling (the so-called "retained β ") transform into a complex martensitic structure which contains a high density of NiAl precipitates.

The κ_I precipitates, which may form in alloys with relatively high iron contents, have a dendritic morphology with dimensions of 20 to 50 μ m. These precipitates are cored and have a composition which varies from iron-rich solid solution to Fe₃Al; this variation in composition is reflected by the existence of a range of crystal structures across individual κ_I particles. The κ_{II} particles, which also have a dendritic morphology with dimensions of 5 to 10 μ m, have a composition based on Fe₃Al and the DO₃ structure. The κ_{III} particles are the product of eutectoidal decomposition and have a lamellar or globular (degenerate lamellar) shape; κ_{III} is based on NiAl and has the B2 structure. The κ_{IV} particles form as relatively small, <2 μ m, equiaxed precipitates in the α -phase. These particles are based on Fe₃Al and have the DO₃ structure.

The precipitates κ_I , κ_{II} , and κ_{III} have the Kurdjumov-Sachs orientation relationship with the α matrix. Small κ_{IV} particles have the Nishiyama-Wasserman orientation relationship with the α matrix, while the larger particles have an orientation relationship which lies between Kurdjumov-Sachs and Nishiyama-Wasserman.

Tempering the as-cast alloy at 675 °C results in the formation of a high density of precipitates in α with the B2 structure based on NiAl.

ACKNOWLEDGMENTS

This work was supported by the Procurement Executive, Ministry of Defence. The EM400T was purchased with the assistance of grants from SERC and NERC.

REFERENCES

1. M. Cook, W.P. Fentiman, and E. Davis: *J. Inst. Metals*, 1952, vol. 80, pp. 419-29.
2. P. Weill-Couly and D. Arnaud: *Fonderie*, 1973, vol. 28, no. 322, pp. 123-35.
3. E. A. Culpan and G. Rose: *J. Mater. Sci.*, 1978, vol. 13, pp. 1647-56.
4. D. M. Lloyd, G. W. Lorimer, and N. Ridley: *Met. Technology*, 1980, vol. 7, pp. 114-19.
5. G. Cliff and G. W. Lorimer: *J. Microscopy*, 1975, vol. 103, pp. 203-07.
6. J. C. Rowlands and T. R. H. M. Brown: Proc. of the 4th International Congress on Marine Corrosion and Fouling, Entibes, Juan-les-Pins, June 1976, Centre de Recherches et d'Études Océanographique, Boulogne, France.
7. H. Warlimont and L. Delaey: *Prog. Mater. Sci.*, 1974, vol. 18, pp. 25-32 and 41-46.
8. R. Thomson and J. O. Edwards: Report MRP/PMRL/76-27(J), Part I, CANMET, Ottawa, Ontario, Canada.
9. C. S. Barrett and T. B. Massalski: *Structure of Metals*, Pergamon Press, 1980, p. 275.
10. A. J. Bradley, W. L. Bragg, and C. Sykes: *J. Iron Steel Inst.*, 1940, vol. 141, pp. 99-109.
11. R. P. Elliott: *Constitution of Binary Alloys, First Supplement*, McGraw-Hill, 1965, p. 36.
12. M. Hansen: *Constitution of Binary Alloys*, McGraw Hill, 1958, p. 90.
13. G. Lutjering and H. Warlimont: *Acta Met.*, 1964, vol. 12, pp. 1460-61.
14. R. Thomson and J. O. Edwards: Report MRP/PMRL/76-28(J), Part II, CANMET, Ottawa, Ontario, Canada.
15. F. Hasan, G. W. Lorimer, and N. Ridley: University of Manchester, unpublished research, 1982.